State of the Art in Electromagnetic Flow Control in Continuous Casting of Steel Slabs: Modeling and Plant Validation

Brian G. Thomas and Rajneesh Chaudhary

Department of Mechanical Science and Engineering,
University of Illinois, 1206 W Green Street, Urbana, 61801, IL, USA

Abstract
Electromagnetic forces are an important tool to control fluid flow in the mold, combined with other casting conditions, nozzle, and mold geometry. Methods include static magnetic fields created by direct current, which apply a braking force in proportion to the flow velocity, and time-varying (travelling) magnetic fields, which actively drive the flow. The potential benefits of using magnetic fields to help control the flow pattern include fewer surface and internal defects, refined microstructure, improved uniformity, fewer inclusions, increased productivity and reduction in mold copper wear, especially at higher casting speeds. Used nonoptimally, however, electromagnetic forces can have the opposite effect, producing detrimental flow patterns and increased quality problems. Numerical models are the best tool for optimizing electromagnetic flow control, but the complexities of transient turbulent flow and the accompanying phenomena which govern defects make accurate predictions very difficult. Thus, validation with analytical solutions, laboratory measurements, and plant measurements is essential. This paper reviews these models and validation methods and shows example findings for a local static field with varying SEN depth. Using the knowledge gained from models and measurements together, electromagnetic forces and other casting parameters can be controlled together to stabilize the fluid flow in the mold cavity, minimize casting defects, and improve quality.

Introduction

Fluid flow in the mold governs the quality of continuous-cast steel, so the mold flow pattern must be controlled within acceptable process windows to avoid excessive surface velocities, high surface waves, meniscus stagnation, shell thinning, inclusion entrapment, and many other problems [1]. Mold fluid flow is inherently turbulent, so in addition to maintaining an optimal time-averaged flow pattern, it is important to achieve a stable flow pattern that minimizes detrimental transient fluctuations. The mold flow pattern should have a reasonably-flat surface profile, with stable meniscus velocities optimized within an acceptable range, to avoid surface defects and slag entrainment. It should also achieve reasonable tangential velocity across the dendritic front while avoiding excessive downward velocity, to minimize internal inclusion entrapment. Decreasing level fluctuations lessens thermal cycling and thermal fatigue of the copper plates, increasing mold life.

These important flow parameters are governed by the flow control system (stopper rod or slide gate), nozzle geometry, (port size, shape, angle, etc.), Submerged Entry Nozzle (SEN) depth, casting speed, strand cross-section dimensions, argon gas injection, slag behavior, and the application of electromagnetics [1]. Among these, magnetic field strength offers a powerful and flexible control parameter that can be varied in real time, and inherently lessens turbulent fluctuations. Different magnetic field configurations have been used to help control the steel flow in continuous casting. Electromagnetic control systems are categorized broadly into two types: 1) EMBr, which uses direct current to maintain a constant Electro-Magnetic field that applies a Braking force in proportion to the flow velocity; and 2) moving-field control, which generates a time varying magnetic field to actively drive the flow, including accelerating, decelerating, or stirring action.

EMBr type systems include local, single-ruler, and double-ruler (FC-mold) configurations. Local EMBr applies a circular shaped magnetic field to small regions on both sides of the nozzle (Fig-1(a)). This region exerts a force on the steel jet passing through it, which slows and deflects the jet [2, 3]. A “ruler-brake” extends the magnetic field region over the whole mold width (Fig-1(b)). Using two such magnetic-field rulers (is more popular because it allows independent control of both surface velocity, and velocity in lower recirculation zone ((Fig-1(c)) [2, 3], while avoiding direct interaction with the jet.

Moving (traveling) magnetic-field systems (Fig-1(d)) can vary between many different modes, including electromagnetic level stabilizer (EMLS) to decelerate the flow, electromagnetic level accelerator (EMLA), electromagnetic stirring (rotational Mold-EMS / EMRS [4], or final-strand-EMS]. These systems offer even more flexibility. Choosing the best configuration and field magnitudes as a function of process conditions is the challenge facing all of these systems.

It is very difficult to measure the flow of hot, opaque molten steel, especially with the interference of applied electro-magnetic fields [5]. Water model experiments cannot incorporate the electromagnetic effects. Thus, investigations of fluid flow in the mold with electromagnetic forces must rely on computational models, supplemented with insights gained from experiments with molten metal. This paper reviews computational and experimental tools to understand and optimize electromagnetics to control fluid flow in the mold in order to improve quality in continuous casting of steel.

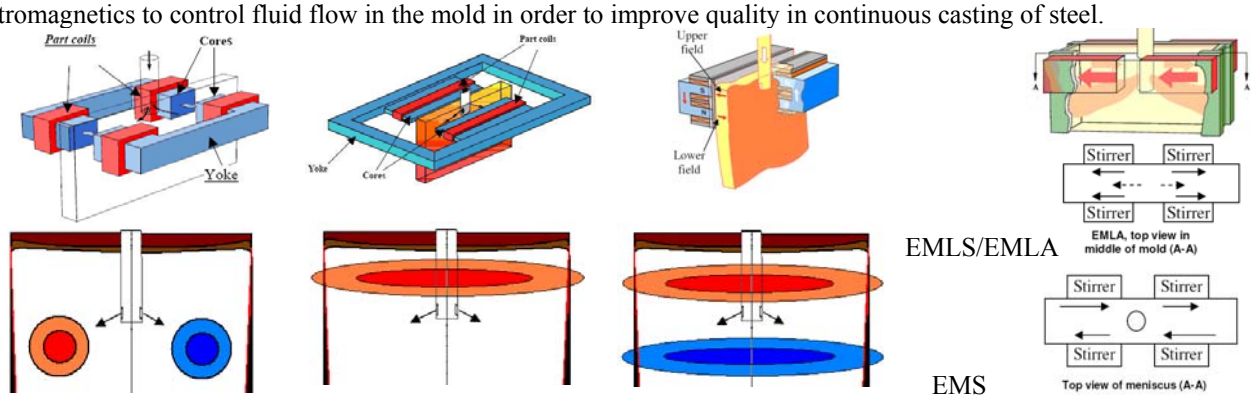

(a) Local EMBr (b) Ruler EMBr (c) Double ruler EMBr (d) Moving field systems

Fig. 1: Various types of electo-magnetic mold flow control systems showing hardware (top) and field shape (below)

Real caster: velocity measurements

Several different methods have been evaluated to measure surface velocity in a harsh molten-metal environment [6-9]. Surface visualization methods, such as photographic analysis of moving variations on the exposed surface are generally prevented by the slow-moving, opaque slag layer that covers the flowing metal. Measuring the force or vibration frequency on a ceramic-covered rod inserted through the top surface of the continuous-casting mold is a recent, popular method to measure velocity [7]. Inserting nail boards is a very simple, yet powerful tool to gain even more information. Nailboard measurements are commonly used to measure the thickness of the molten slag layer, and the liquid level profile [8].

The nailboard test is performed by dipping one or two rows of 5~15 steel nails and aluminum wires straight down through the slag layer into the top surface of the mold, as shown in Fig. 2. They should remain immersed for 3-4s, in order to solidify a thin skull of metal onto the end of each nail. Excessive immersion time may cause problems such as remelting the skull or solidifying the steel surface in the mold. With electromagnetic braking, testing is easier if the nails are stainless steel, in order to avoid electromagnetic forces acting on the nails. After removal, the shape of the lump of steel that has solidified on the end of each nail, and the aluminum wire lengths are measured.

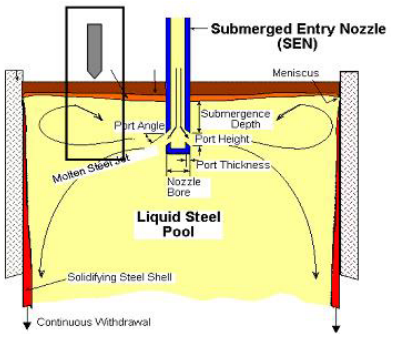

Fig. 2: Continuous casting mold showing steel flow, top-surface slag layers, and location of nail-board insertion

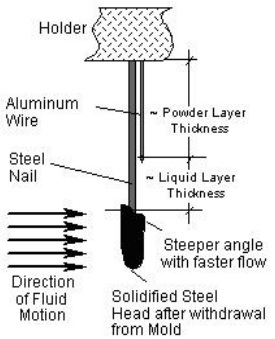

Fig. 3: Nailboard method to measure steel surface speed and direction

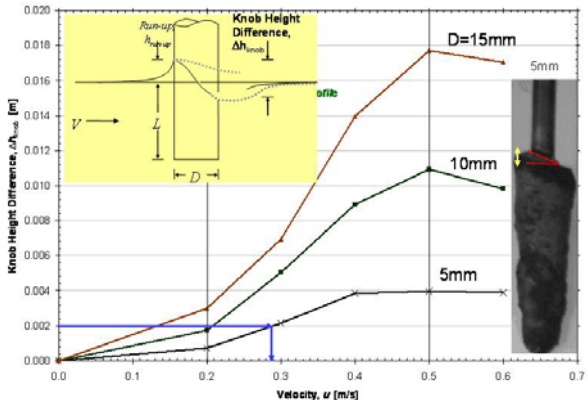

Fig. 4: Nail photo showing measurement of solidified knob

Fig. 3 shows a schematic of a nail with the lump. Recently, a carefully-validated computational model was used to determine a relation (Fig. 4) to correlate knob height difference, Δh, and nail diameter, D, to surface velocity of the molten steel across the top of the mold [9]. The model features 3-D turbulent flow in the steel coupled with laminar flow in the slag

layer, and two free surface computations using the SPINES method in the finite-element CFD package, FIDAP. The calculated knob height difference varies with the nail diameter the fluid densities, viscosity, and interfacial tension, so the interface between the molten steel and the slag layer is much different than in a water model. Once the knob height is measured for a given diameter nail, Fig. 4 can be used to find free surface velocity [9].

Real caster: free-surface level measurements

Oscillation marks are small depressions in the surface of a steel slab caused by partial freezing of the meniscus during a mold oscillation cycle [10]. These marks show the shape of the meniscus and free surface at the instant in time they are formed. This gives another opportunity for validation of a computational model; the simulated meniscus shape caused by the fluid flow pattern can be compared with the meniscus shape obtained from oscillation marks. Portions of the slab surface can be sandblasted to remove surface scale to clearly reveal the oscillation marks. Fig-6 shows typical oscillation marks, outlined in dark marker to increase visibility. Photographs with a ruler to provide scale can be expanded and measured to obtain the deviation in oscillation mark position relative to a horizontal flat meniscus.

Mathematical modeling

Computer simulations can reveal the flow pattern for the conditions of interest, provided that all of the relevant phenomena are properly incorporated, including the effects of momentum (controlled by nozzle design, casting speed, etc.), gas-bubbles, and electromagnetics. Other complicating phenomena include free surface effects (needing a VOF model), particle transport and entrapment, solidification, and sometimes buoyancy (both thermal and solutal) [5].

Modeling single-phase flow

Single-phase steel flow in the mold is governed by well-known N-S (Navier-Stokes) equations for momentum transport, together with the continuity equation for mass conservation [15]. As the flow is dominated by inertia, (high Reynolds number), turbulence develops with different scales. In order to capture all these scales, the N-S equations need to be integrated with a very fine mesh and very small time-steps [5], which is called DNS (Direct Numerical Simulation) and is practically impossible in continuous casting molds. Therefore, as a short-cut, LES (Large Eddy Simulation) is used to capture the larger scales and account for scales smaller than subgrid with a subgrid-scale model [11-12]. Even LES is very computationally-intensive, so the RANS (Reynolds Averaged Navier Stokes) approach to solve the time averaged-N-S equations is the most popular and efficient approach [13]. The RANS approach needs a turbulence model. One of the many variants is the k-ε model which solves two additional PDEs for transport of k and ε to modify the viscosity [13-15]. Using special "wall functions" for boundary conditions at walls allows a coarse mesh to capture the steep gradients close to the wall, which decreases computational cost [11]. The RANS model compares well with time-averaged results of both DNS and LES models for turbulent flow in a continuous casting mold cavity [16].

Modeling with multiphase flow effects

Argon gas is usually injected into the nozzle, slide-gate, and / or stopper rod to avoid nozzle clogging and to help with inclusion removal. This gas requires a multiphase flow model, which is further complicated by solid inclusion particles in the molten steel. Multiphase models have different reference frames and methodologies for coupling between phases. Reference frames include Eulerian, Lagrangian and hybrid combinations. Fluid flows through Eulerian domains, which are fixed in the laboratory frame of reference. Lagrangian methods follow the particles. Eulerian reference frames have two main coupling methods: mixture models [17] and separated fluid models [18-19]. In mixture models, the velocities in different phases differ by a constant "slip-velocity" [17] This approach is reasonable for dilute steel-argon flows, except where gas pockets collect, such as above the nozzle ports or behind the slide-gate region. With high gas fractions, separated fluid models are better. This approach solves a separate set of flow equations for each phase. This is accurate for a small range in gas bubble diameter, but becomes computationally intensive when modeling multiple equation sets to represent different size ranges. To overcome this difficulty, Lagrangian techniques [20] track each individual bubble transiently, which is both accurate and cost-effective if the number of bubbles is not excessive. In addition to solving steel-argon two-phase flow, the Lagrangian approach is popular for tracking inclusion particle transport and entrapment in the solidifying shell, causing defects in the cast product. All of these methods have been used successfully to model steel flow in continuous casting molds.

Modeling with electromagnetic effects

Extensive work has been carried out to investigate both static and moving fields on fluid flow in steel continuous casting [21-22]. Experimental and numerical studies were performed on a slab caster with a double-ruler electromagnetic field and

improvement in surface and internal quality was reported [23]. The steel jet exiting the SEN nozzles was modeled to bypass around the strong central region of a local static magnetic field and thus cause non-uniform flow [24]. The effect of EMS on multiphase flow in the mold was studies with experiments in mercury and simulations using a two-fluid model. Lorentz force was found to suppress the effect of argon gas in the mold [25]. Both argon gas and EMBr were found to assist inclusion removal and to suppress free surface fluctuations [26].

The first step in modeling flow in the mold with electromagnetic effects is to determine the external applied magnetic field, B_0, which can either be measured or calculated using the A-ϕ method given elsewhere [27-28]. Then, in addition to the flow model equations, coupled Maxwell's equations, and Ohm's law must be solved. The movement of the conducting steel through the applied magnetic field induces a current, which generates a Lorentz force [29] that tends to oppose the flow. Two different modeling approaches are used to model fluid flow with MHD, depending on the importance of coupling between the applied and induced magnetic fields.

When the Magnetic Reynolds number, $\mathrm{Re}_m = vL(\mu\sigma)$, is <1 (such as for liquid metals), the induced magnetic field is negligible relative to the applied field, so the "electric potential method" is most efficient. Based on Ohm's law and conservation of charge, coupled equations for electric potential, ϕ, and Lorentz force, $\vec{F}_L$ can be solved as follows [29].

$$\nabla^2\phi = \nabla\cdot\left(\vec{v}\times\vec{B}_0\right) \text{ and } \vec{F}_L = \sigma\left(-\nabla\phi + \vec{v}\times\vec{B}_0\right)\times\vec{B}_0 \qquad (1)$$

In time varying fields, and when the induced current is significant, (Re_m >1), the "magnetic induction" method is best. Maxwell's equations are combined with Ohm's law to obtain a transport equation for the induced magnetic field, $\vec{b}$ in terms of the total field, $\vec{B}$ and the current density, $\vec{J}$ [29].

$$\frac{\partial\vec{b}}{\partial t} + (\vec{v}\cdot\nabla)\vec{b} = \frac{1}{\mu\sigma}\nabla^2\vec{b} + \left(\left(\vec{B}_o + \vec{b}\right)\cdot\nabla\right)\vec{v} - (\vec{v}\cdot\nabla)\vec{B}_o - \frac{\partial\vec{B}_0}{\partial t} + \frac{1}{\mu\sigma}\nabla^2\vec{B}_0 \qquad (2)$$

$$\vec{B} = \vec{B}_o + \vec{b}\ ; \qquad \vec{J} = \nabla\times\vec{B}/\mu\ ; \qquad \vec{F}_L = \vec{J}\times\vec{B} \qquad (3)$$

In both methods, the Lorentz force is applied as a source term into the flow equations to alter the fluid velocities.

Model validation and sample results

Numerical and experimental studies were performed to optimize flow in a thin-slab caster with a local static EMBr field, and varying SEN depth [30]. The steady-state, 3-dimensional, incompressible, Navier-Stokes equations, the continuity equation, and the standard k- and ε- equations were solved using FLUENT [16]. To model the effect of shell solidification, mass and momentum sink terms can be added to the continuity and momentum equations. Details on these sink terms are given elsewhere [31].

The magnetic field was measured using a Gauss meter in the empty mold, assuming it was the same in operation. This approximation is reasonable because copper is a paramagnetic material and molten steel loses its magnetic properties and behaves like a paramagnetic material (above Curie temp. ~600 ^{0}C) [4]. Magnetic field strength through the thickness of the mold was measured to vary by a maximum of only 3%.

With known external field, the magnetic induction method of FLUENT [32] was employed for turbulent steel flow-magnetic field coupling. The model was validated with both measured velocities using nailboard tests (Fig. 5) and surface shape from oscillation mark profiles (Fig. 6) and then was extended for parametric studies with different SEN depths and field strengths. Fig. 5 compares the measured and predicted velocity at the mold mid plane with 300-mm SEN depth and the maximum field strength of 0.355 T. The results match surprisingly well both near the narrow face and near the SEN.

Fig. 6 compares the calculated meniscus profile with eight separate oscillation marks. The oscillation marks were graphed such that the total "area under the curve" of each oscillation mark is equal to zero. The calculated profile roughly matches that of the oscillation marks. The trend of a high wave at the narrow face that slopes downward and stabilizes about halfway across the wide face before sloping slightly upward near the SEN is witnessed in both the experimental and numerical cases. The scale of the numerically calculated profile also matches that of the oscillation marks. The match is not exact, however, perhaps because the oscillation marks are transient by nature, as indicated by the variations between the

eight oscillation marks. The standing wave heights range from 2.25mm to 6.0mm. The average measured height is 4.41mm, which is only 0.85mm smaller than the calculation. This shows that the model can roughly predict the average surface profile, both qualitatively and quantitatively, which is the best that can be expected from a steady-state model.

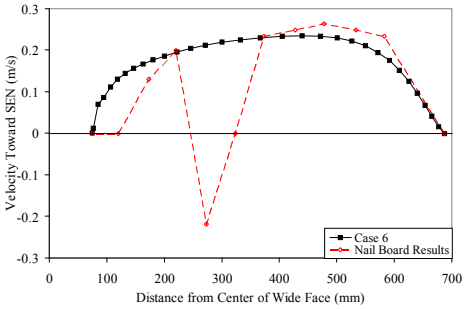

Fig. 5: Comparison of calculated and experimental meniscus velocity

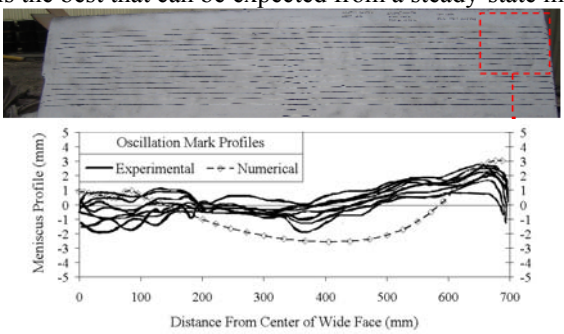

Fig. 6: Comparison of oscillation marks on slab surface (top) with calculated free-surface profile

Fig. 7 shows velocity vectors computed at the mold mid plane with circles showing the applied field. The jet exiting the nozzle travels across the mold cavity, impinges on the narrow face, splits into upward and downward jets, creating the classic upper and lower recirculation zones of a double-roll flow pattern. In the upper recirculation zone, fluid flows up the narrow face, back across the top surface, and down the SEN wall, to rejoin the jet exiting the nozzle. The brake causes some of the secondary jet flowing up the narrow face to split off early and flow back across the mold just above the brake region, altering velocities in the upper recirculation region. In the lower recirculation zone, fluid flows down the narrow face, across the mold cavity width, and up the center of the mold cavity. The lower recirculation zone is much larger and has lower velocities than the upper zone, because it is not confined. The upper zone is constrained by the top surface and the jet exiting the SEN, which tends to bend the jet slightly upwards.

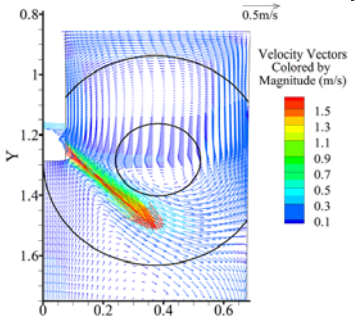

Fig. 7: Velocity vectors on the mold wide face centerplane (SEN depth=300 mm and 0.355 T field), with outer circle showing extent of EMBr field, and inner circle showing region of strongest field.

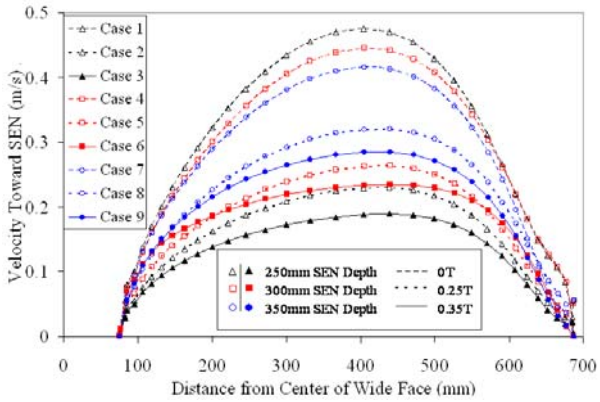

Fig. 8: Velocity across top surface toward the SEN

Velocity across the top surface is compared for all nine cases in Fig. 8, which shows velocity toward the SEN on a line across the wide-face centerplane 10mm below the meniscus. A parabolic velocity profile is seen, with a maximum about 450mm from the mold center. Without EMBr, surface velocity decreases with increasing SEN depth. With EMBr, this trend reverses, because the jet drops below the EMBr region, and maintains its momentum.

The parametric study of the combined effects of EMBr and SEN depth revealed the following:

1. Increasing EMBr field strength at constant SEN depth causes a steeper downward jet angle, lower impingement point, lower velocities deep in the caster, expanded weaker upper recirculation zone with lower top surface velocity and flatter meniscus profile.
2. Increasing SEN Depth without EMBr has almost the same effects as increasing EMBr listed above. The only exception is that jet dissipation is not increased, so downward velocity increases at depths more than 0.5m into the mold cavity.
3. Increasing SEN Depth with EMBr has almost exactly the opposite effects as increasing EMBr. This is because the jet tends to move below the EMBr region, so is less affected by the EMBr field.

Conclusions

This paper summarizes different ways to alter the flow pattern in the steel continuous casting mold using electromagnetic forces, and the computational methods used to study them. Computational models always require rigorous validation with plant measurements before extending their predictions to meaningful parametric studies. To this end, nailboard velocity measurement and oscillation marks for free-surface profiling are simple but powerful practical ways to measure, the surface flow pattern. Due to the transient nature of turbulent flow, such measurements should be repeated many times for reliability.

Electromagnetic forces are just one of several parameters which control the flow pattern. Nozzle geometry, gas injection, and MHD must all be optimized together for a given speed and section size, so there is no universal best field configuration.

An accurate, validated computational model is a powerful and inexpensive tool to assist in designing MHD to help control the flow pattern in steel continuous casting. The RANS approach with MHD can be effectively used to predict and optimize the effect of magnetic field on transient velocity and level fluctuations in the mold to produce high quality steel.

Acknowledgements

The authors gratefully thank Kevin Cukierski for the electromagnetic study, Bret Rietow for the nailboard velocity work, Ron O'Malley for the measurements at Nucor, Decatur, AL, and the Continuous Casting Consortium for funding.

References

[1] B. G. Thomas, Chapter 14. Fluid Flow in the mold, in Making, Shaping and Treating of Steel, A.W. Cramb, Editor. 2003, AISE Steel Foundation: Pittsburgh, PA.

[2] A. Idogawa, Y. Kitano and H. Tozawa: Kawasaki Steel Tech. Rep., 1996, 35, 74–81.

[3] H. Harada, T. Toh, T. Ishii, K. Kaneko and E. Takeuchi: ISIJ Int., 2001, 41, 1236–1244.

[4] S. Kunstreich, Electromagnetic stirring for continuous casting-Part-I, La Revue de Métallurgie-CIT, Avril 2003.

[5] Brian G. Thomas, Lifeng Zhang : ISIJ International, 2001, Vol.41, No.10, pp.1181-1193.

[6] Argyropoulos, S.A., Measuring velocity in high-temperature liquid metals: a review. Scand. J. Metall., 2000. 30.

[7] J. Kubota: in *Mold Operation for Quality and Productivity*, Cramb, Szekeres, eds. Iron & Steel Soc., 1991.

[8] P.H. Dauby, W.H. Emling, and R. Sobolewski,: Ironmaker and Steelmaker, 1986. 13(Feb): p. 28-36.

[9] Rietow, B. and B.G. Thomas, AISTech 2008 Steelmaking Conference Proc., (Pittsburgh, PA, May 5-8, 2008).

[10] Takeuchi, E and J. K. Brimacombe, : Metall. Trans. B, 1984, Vol. 15B, No. 3, pp. 493-509.

[11] J. Smagorinsky: Monthly Weather Review, (1963), 91, 99.

[12] S. Sivaramakrishnan, B. G. Thomas and S. P. Vanka:, in Materials Processing in the Computer Age, 3, V. Voller and H. Henein, eds., TMS, Warrendale, PA, (2000), 189-198.

[13] B. E. Launder and D. B. Spalding: Computer Methods in Applied Mechanics and Engr, (1974),13 (3), 269.

[14] B. E. Launder and D. B. Spalding, Mathematical Models of Turbulence. 1972: London Academic Press.

[15] B. G. Thomas, Chapter 5. Modeling of Continuous Casting, in Making, Shaping and Treating of Steel, A.W. Cramb, Editor. 2003, AISE Steel Foundation: Pittsburgh, PA.

[16] Thomas, B.G., Yuan, Q., Sivaramakrishnan, S., Shi, T., Vanka, S.P., and Assar, M:ISIJ Int.,2001,41(10):.

[17] B. G. Thomas, X. Huang and R. C. Sussman: Metall. Trans. B, 25B (1994), No. 4, 527.

[18] H. Bai and B. G. Thomas: Metall. Mater. Trans. B, 32B (2001), No.2, 253.

[19] H. Bai and B. G. Thomas: Metall. Mater. Trans. B, 32B (2001), No. 2, 269.

[20] N. Kubo, J. Kubota, M. Suzuki and T. Ishii: Nippon Steel Tech. Rep., (1998), No. 164, 1.

[21] K.-H. Spitzer, M. Dubke and K. Schwerdtfeger: Metall. Mater.Trans. B, 17B (1986), No. 2, 119.

[22] N. Genma, T. Soejima, T. Saito, M. Kimura, Y. Kaihara, H. Fukumoto and K. Ayata: ISIJ Int., 29 (1989), No. 12.

[23] Idogawa A., Sugizawa M., Takeuchi S., Sorimachi K., and Fujii T.: Mats Sc and Eng., A173, (1993) 293-297.

[24] Y. Hwang, P. Cha, H. Nam, K. Moon and J. Yoon: ISIJ Int., 37 (1997), No. 7, 659.

[25] B. Li, T. Okane and T. Umeda: Metall. Mater. Trans. B, 31B (2000), No. 6, 1491.

[26] H. Shen, B. Liu and L.Wang: : International Journal of CastMetals Research, 2005 Vol. 18, No 4.

[27] T. Ueyama, K. Shinkura, and R. Ueda, IEEE Trans. Magn., vol. 25, no. 5, pp. 4153–4155, 1989.

[28] Ryu Hirayama, Keisuke Fujisaki and Takahiro Yamada: IEEE Trans. Magn., vol. 40, no. 4, 2004

[29] R. Moreau. Magnetohydrodynamics. Kluwer Academic Publishers, 1990.

[30] Kevin Cukierski and Brian G. Thomas,: Metall. Mater. Trans B, Vol. 39, No. 1, Feb 2008.

[31] Chaudhary R., Lee Go-Gi, Thomas B. G., and Kim S-H: Met. and Mat Trans B, Vol. 39, No-6, Dec 2008.

[32] FLUENT6.3-Manual (2007), ANSYS Inc., 10 Cavendish Court, Lebanon, NH, USA.